Plasticity and learning in a network of coupled phase oscillators

Philip Seliger, Stephen C. Young, and Lev S. Tsimring
Institute for Nonlinear Science, University of California, San Diego, La Jolla, California 92093-0402
(Received 23 October 2001; published 26 March 2002)

A generalized Kuramoto model of coupled phase oscillators with a slow varying coupling matrix is studied. The dynamics of the coupling coefficients is driven by the phase difference of pairs of oscillators in such a way that the coupling strengthens for synchronized oscillators and weakens for nonsynchronized pairs. The system possesses a family of stable solutions corresponding to synchronized clusters of different sizes. A particular cluster can be formed by applying external driving at a given frequency to a group of oscillators. Once established, the synchronized state is robust against noise and small variations in natural frequencies. The phase differences between oscillators within the synchronized cluster can be used for information storage and retrieval.

DOI: 10.1103/PhysRevE.65.041906 PACS number(s): 87.18.Sn, 05.45.Xt, 07.05.Mh, 87.19.La

I. INTRODUCTION

The mechanisms of adaptation and learning in natural and artificial systems are a subject of paramount interest in the neuroscience. Most of the experimental evidence points to the synaptic modification as the physiological basis of the long-term memory [1,2]. Hebb [3] was the first who suggested that the synaptic coupling between two neurons is enhanced if both neurons are simultaneously active. Recent experimental data suggests that the synaptic connections are strengthened [long-term potentiation (LTP)] or weakened [long-term depression (LTD)] depending on the precise relative timing between presynaptic and postsynaptic spikes [2,4,5].

Many current theoretical studies of learning in neural systems are based on the quasistatic Hopfield model [6] utilizing McCulloch-Pitts neuronal units or simple ''integrate-and-fire'' models of neurons coupled via synapses that accumulate the presynaptic activity (spikes from other neurons) into a growing membrane potential of a neuron [7]. The latter generates its own spike (''fires'') once the membrane potential exceeds a certain threshold. The synaptic strength is in fact not fixed, but changes in response to external stimuli and/or interneural dynamics. Various models based on this general picture [8,9], have been shown to yield differential Hebbian learning rules.

A complimentary approach to modeling neuronal activity involves replacing neurons by periodic oscillators. Indeed, rhythmic activity plays an important role in many neuronal systems and functions, including central pattern generators, visual and olfactory systems, etc. [10]. Neural networks can often be described as networks of coupled oscillators, so the role of relative spike timing is played by the phases of individual oscillators (see, for example, [11–14]). Close to the Hopf bifurcation, the dynamics of the array of coupled oscillators can be described by the Landau-Stewart equations for complex amplitudes of the oscillators. Furthermore, one can reduce the dynamics of the oscillators to the pure phase dynamics by assuming that the coupling is weak, and the amplitude of oscillations is slaved to the phase variations. In fact, the phase dynamics description may still be valid even away from the Hopf bifurcation point, where the Landau-Stewart description is not applicable. This idea was first put forth by Winfree [15] and later developed by Kuramoto [16] and others [17]. The original Kuramoto model, in which the coupling coefficients were chosen as fixed and equal, allowed for an elegant analytical treatment within the mean-field approximation. It was shown that the system of globally coupled oscillators with nonidentical frequencies exhibits a second-order phase transition as the coupling strength is increased above some critical value.

In subsequent work, more complex coupling functions were considered [14,18,19]. It was shown that depending on the choice of the connectivity matrix, synchronized states with a nontrivial phase relationship among the oscillators can emerge. Networks of coupled phase oscillators with an appropriately tuned coupling matrix were shown to have neurocomputing properties similar to those of the classical Hopfield network, with an important distinction that memorized patterns are stored in the form of relative phases of synchronized oscillators rather than in static equilibria.

In those studies, the connectivity matrix, however, complicated, was imposed externally to achieve the desired network dynamics. In fact, in order to achieve certain behavior (for example, to memorize an image), in a system of N neurons, N^2 coupling coefficients have to be specified. This would present significant difficulties in operating such a system at a large N. In biological neural networks this task is not assigned to any central control unit, but is performed in a distributed manner via the mechanism of synaptic plasticity, i.e., long-term potentiation or depression of synapses in response to the dynamics of presynaptic and postsynaptic neurons [2,8]. External stimuli directly affect only the dynamics of individual neurons and not their connections, while the synaptic plasticity is a result of the interneuronal interactions. This evolution of connectivity matrix has been introduced in Ref. [13] for the Landau-Stewart model of coupled oscillators, however, no analysis of the joint dynamics of the network of oscillators *and* the connectivity matrix has been presented. In this paper, we study the simplest possible model of this process, based on the generalization of the Kuramoto model. In particular, we assume that the coupling

coefficient for a link between two oscillators is a slow function of their phase difference.

The paper is organized as follows. In Sec. II we introduce the generalized Kuramoto model with additional equations describing the slow evolution of the coupling matrix. In Sec. III, a simple case of two coupled oscillators is investigated. We show that for a large separation of time scales of fast and slow motions, the system is bistable: depending on initial conditions, oscillators can be either synchronized or nonsynchronized. In Secs. IV and V, we study the existence and stability of the family of synchronized cluster solutions in the continuum limit $N\to\infty$. In Sec. VI, we show that the generalized Kuramoto system can serve as a very simple model of learning and memory. Information is stored within the synchronized cluster in the form of phase differences between oscillators. Section VII summarizes our conclusions.

II. MODEL

Let us consider the dynamics of an ensemble of N coupled phase oscillators

$$\dot{\phi}_i=\omega_i-\frac{1}{N}\sum_{j=1}^{N}K_{ij}F(\phi_i-\phi_j). \tag{1}$$

Here ω_i are natural frequencies and ϕ_i are phases of individual oscillators, $F(\phi)$ is a 2π-periodic coupling function, and K_{ij} is the $N\times N$ matrix of coupling coefficients.

In order to include the mechanism of adaptation into model (1), we assume that an element of the coupling matrix describing interaction between two oscillators, i and j, is controlled by the following equation:

$$\dot{K}_{ij}=\epsilon[G(\phi_i-\phi_j)-K_{ij}], \tag{2}$$

where $G(\phi)$ is a 2π-periodic function of its argument. The particular form of the coupling function $F(\phi)$ and adaptation function $G(\phi)$ can be derived from the underlying equations describing the dynamics of oscillators through the reduction to the phase description. Following Kuramoto [16], we choose the simplest possible periodic function $F(\phi)=\sin\phi$. Furthermore, we choose the adaptation function $G(\phi)=\alpha\cos\phi$. This choice implies that the coupling coefficient grows fastest for two oscillators that are in phase and decays fastest for out-of-phase oscillators. This form of the adaptation function directly corresponds to the Hebbian rule of learning [3] and has been proposed before [13] in a similar context. There are certain indications in the biological literature (see Ref. [2]) that the maximal LTP and LTD correspond to small positive and negative phase shifts between presynaptic and postsynaptic neuronal oscillations. However, we are going to ignore this complication in our model for the sake of simplicity. With the chosen functions, our model becomes

$$\dot{\phi}_i=\omega_i-\frac{1}{N}\sum_{j=1}^{N}K_{ij}\sin(\phi_i-\phi_j), \tag{3}$$

$$\dot{K}_{ij}=\epsilon[\alpha\cos(\phi_i-\phi_j)-K_{ij}]. \tag{4}$$

For small ϵ, the dynamics of the coupling coefficients is slow, and one can expect that for two oscillators which are nonsynchronized, the driving term $\alpha\cos(\phi_i-\phi_j)$ is oscillating around zero, and the resultant coupling coefficient is also oscillating around zero and is small $O(\epsilon)$. On the other hand, a pair of synchronized oscillators produces a constant nonzero driving for the corresponding coupling coefficient, and, therefore, for large enough α, the connection between the two will be strengthened. Thus, we anticipate a multistable behavior, when a group of oscillators can either be stably synchronized or nonsynchronized depending on the initial conditions for their coupling coefficient. To illustrate this point, we first consider a simple case of two oscillators symmetrically coupled through a single link.

III. TWO COUPLED OSCILLATORS

In this case model (3) and (4) reduces to a set of two coupled equations,

$$\dot{\phi}=\Delta\omega-K\sin\phi,$$

$$\dot{K}=\epsilon(\alpha\cos\phi-K). \tag{5}$$

Here $\phi=\phi_1-\phi_2$, $K=K_{12}=K_{21}$, and $\Delta\omega=\omega_1-\omega_2$. By introducing new variables $\tilde{t}=\Delta\omega t$, $\tilde{K}=K/\Delta\omega$, $\tilde{\alpha}=\alpha/\Delta\omega$, $\tilde{\epsilon}=\epsilon/\Delta\omega$, system (5) is simplified to

$$\dot{\phi}=1-\tilde{K}\sin\phi,$$

$$\dot{\tilde{K}}=\tilde{\epsilon}(\tilde{\alpha}\cos\phi-\tilde{K}). \tag{6}$$

The nullclines of this system $\tilde{K}=\tilde{\alpha}\cos\phi$ and $\tilde{K}=1/\sin\phi$ intersect at $\tilde{\alpha}>\tilde{\alpha}_c=2$. In this case, within each period of the relative phase ϕ, there are four intersections corresponding to two stable and two unstable fixed points [see Figs. 2(b) and 2(c)]. For small $\tilde{\epsilon}$, the dynamics of the system can be separated into fast and slow motions. If initial value $\tilde{K}_0>1$, the phase variable ϕ rapidly approaches the quasistatic value $\arcsin\tilde{K}_0^{-1}$ corresponding to the nullcline, without any significant change of K. Then, depending on whether $\tilde{K}_0$ is greater or smaller than the value $\tilde{K}_u$ corresponding to the unstable fixed point, the solution either slowly approaches the stable fixed point $\tilde{K}_s$ (synchronized regime), or it reaches the minimum of the nullcline and then branches off to infinity along the fast trajectory. The same occurs if $\tilde{K}_0<1$. This corresponds to the regime of nonsynchronized oscillations. For larger values of $\tilde{\epsilon}$, the dynamics can no longer be reduced to fast and slow motions. Moreover, for any fixed $\tilde{\alpha}>\tilde{\alpha}_c$, there exists some critical value of $\tilde{\epsilon}_c$ such that at $\tilde{\epsilon}>\tilde{\epsilon}_c$ there are no unbounded solutions corresponding to the nonsynchronized motion. On the other hand, if $\tilde{\alpha}<\tilde{\alpha}_c$, there are no fixed points corresponding to

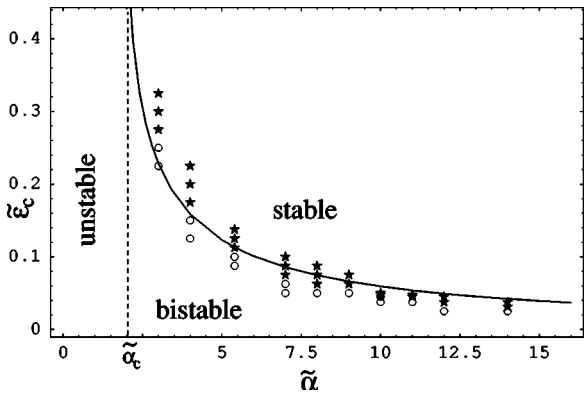

FIG. 1. Phase diagram $\tilde{\epsilon}_c(\tilde{\alpha})$ for the model of two coupled oscillators (6). Symbols show the results of numerical simulations with 50 uniformly distributed oscillators. Circles correspond to the nonsynchronized regime, and stars indicate an onset of synchronization of pairs of oscillators, which usually precedes spontaneous cluster formation.

the synchronized solutions, and the oscillators are desynchronized for any values of ϵ. Figures 2(b) and 2(c) show the structure of the phase plane for system (6) for $\tilde{\epsilon}>\tilde{\epsilon}_c$ and $\tilde{\epsilon}<\tilde{\epsilon}_c$, respectively. Figure 1 shows the dependence of $\tilde{\epsilon}_c$ vs $\tilde{\alpha}$. As expected, $\tilde{\epsilon}_c$ diverges as $\tilde{\alpha}\to\tilde{\alpha}_c+$. This line together with vertical line $\tilde{\alpha}=\tilde{\alpha}_c$ divides the parameter plane into three regions. For $\tilde{\alpha}<\tilde{\alpha}_c$, there can only be nonsynchronized solutions [Fig. 2(a)], for $\tilde{\alpha}>\tilde{\alpha}_c, \tilde{\epsilon}>\tilde{\epsilon}_c$ there are only synchronized solutions [Fig. 2(b)], and for $\tilde{\alpha}>\tilde{\alpha}_c, \tilde{\epsilon}<\tilde{\epsilon}_c$, there is a bistable state when both desynchronized and synchronized regimes are stable [Fig. 2(c)].

The results of this section can be applied to a more generic case of many coupled oscillators. Indeed, as ϵ and/or α is increased, the spontaneous clustering usually begins from synchronization of pairs of neighboring oscillators. For this process, the coupling between these oscillators and other oscillators can be neglected. Symbols in Fig. 1 show the results of numerical experiments with a population of 50 oscillators uniformly distributed within a range $\Delta\Omega=1$ starting from small randomized initial coupling K_{ij}. The bifurcation to random pairing of oscillators that precedes the cluster formation, occurs close to the theoretical line predicted for a simple case of two coupled oscillators.

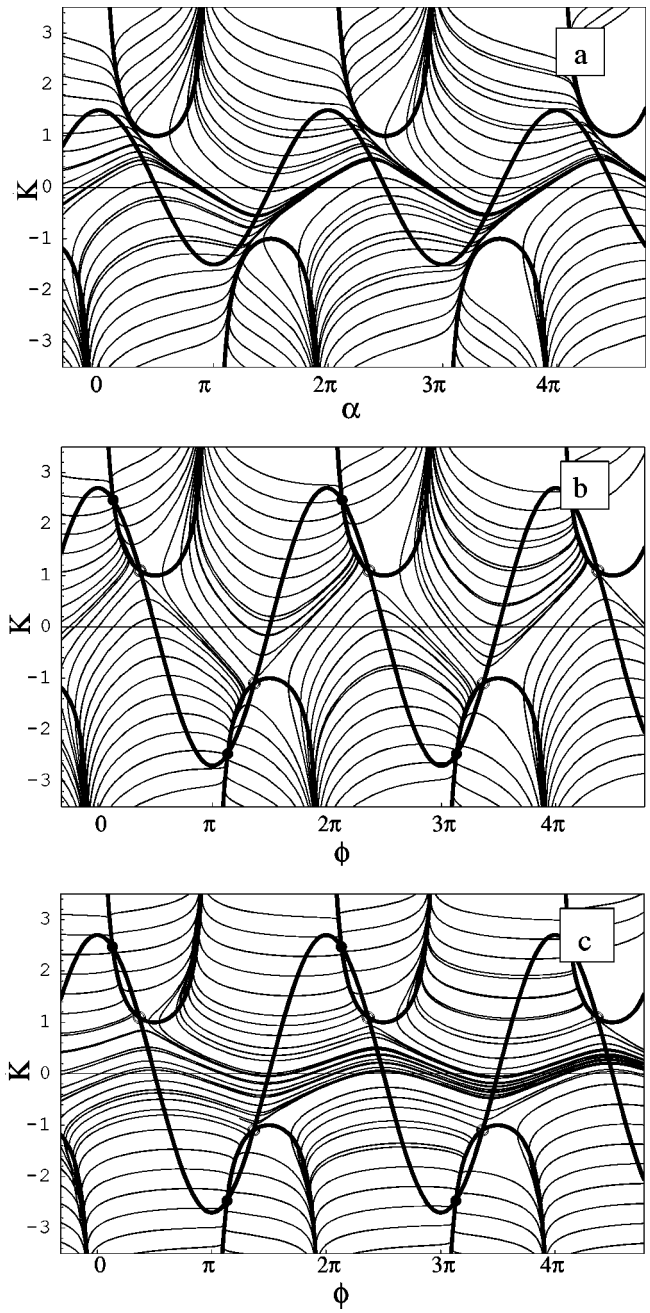

FIG. 2. Phase plane of Eqs. (6): (a) for $\tilde{\alpha}<\tilde{\alpha}_c$ there are no fixed points corresponding to synchronized regime; (b) for $\tilde{\alpha}=2.7$ and $\tilde{\epsilon}=0.33$ all initial conditions lead to stable fixed points; (c) for $\tilde{\alpha}=2.7$ and $\tilde{\epsilon}=0.1$ unbounded solutions coexist with fixed points.

IV. MANY COUPLED OSCILLATORS: STATIONARY STATES

In this section we return to the dynamics of the original model (3) and (4). As was pointed out in Sec. II, for small ϵ, in the asymptotic regime the coupling coefficients are either nonstationary but small (for two oscillators operating at different frequencies) or fixed for two oscillators that are synchronized. So, in the limit $\epsilon\to 0$, we can neglect all K_{ij} for nonsynchronized oscillators, and define $K_{ij}=\alpha\cos(\phi_i-\phi_j)$ for synchronized oscillators. Substituting this into Eq. (3), we obtain for oscillators within a cluster,

$$\dot{\phi}_i=\omega_i-\frac{\alpha}{2N}\sum_{j=1}^{N_c}\sin[2(\phi_i-\phi_j)], \tag{7}$$

where unlike Ref. [16] summation only applies to oscillators within the same cluster, and $\dot{\phi}_i=\omega_i$ for oscillators outside synchronized cluster. It is easy to see that Eq. (7) is formally equivalent to the Kuramoto model for the double phases $2\phi_i$.

One can investigate this model in the mean-field limit $N \to \infty$ using the order parameter method [16]. In this case, the complex order parameter reads

$$\tau e^{2i\theta} = \lim_{N\to\infty} N^{-1} \sum_{i=1}^{N_c} e^{2i\psi_i} = \int_{-\pi}^{\pi} n(\psi) e^{2i\psi} d\psi, \qquad (8)$$

where $\psi = \phi - \Omega t$, Ω is the frequency of the synchronized cluster, and $n(\psi)$ is the phase distribution of the oscillators in the population that belong to the cluster. The phases of the oscillators inside the cluster are given by

$$\psi_i = \theta + \frac{1}{2}\arcsin\left(\frac{2(\omega_i - \Omega)}{\alpha\tau}\right) \qquad (9)$$

and the phase distribution $n(\psi)$ can be easily expressed via the frequency distribution of the synchronized oscillators $g(\omega)$,

$$n(\psi) = \begin{cases} \alpha\tau g\left(\dfrac{\alpha\tau}{2}\sin 2(\psi-\theta) + \Omega\right)\cos[2(\psi-\theta)] & \text{for } B < 2(\psi-\theta) < A \\ 0, \quad \text{outside} \end{cases} \qquad (10)$$

where A, B determine size and position of the synchronized cluster, $(-\pi/2 < B < A < \pi/2)$. Substituting Eq. (10) into Eq. (8), we obtain the equation for the magnitude of the order parameter τ,

$$\frac{\alpha}{2}\int_B^A g\left(\frac{\alpha\tau}{2}\sin x + \Omega\right)\cos x\, e^{ix} dx = 1. \qquad (11)$$

The frequency spread inside the synchronized cluster is determined by the formula

$$\Delta\Omega_c = \frac{\alpha\tau}{2}(\sin A - \sin B), \qquad (12)$$

which follows directly from Eq. (9). Thus, this system exhibits degeneracy so that a variety of synchronized states can be formed depending on initial conditions. It is particularly evident for the uniform distribution of oscillator frequencies within frequency interval $\Delta\Omega$, $g(\omega) = \Delta\Omega^{-1}$. In this case, the cluster size drops out, the limits of integration are symmetric, $B = -A$, and we arrive at

$$\frac{\alpha}{2\Delta\Omega}\int_{-A}^{A} \cos x\, e^{ix} dx = 1, \qquad (13)$$

which reduces to an algebraic equation for phase width of the cluster A,

$$A + \frac{1}{2}\sin(2A) = \frac{2\Delta\Omega}{\alpha}. \qquad (14)$$

The phase width of the cluster A depends only on $\alpha/\Delta\Omega$ and does not depend on the cluster size τ. This dependence is shown in Fig. 3. For large α, $A \approx \Delta\Omega/\alpha$. At $\alpha \to \alpha_0 = 4\pi^{-1}\Delta\Omega$, $A \to \pi/2$. The frequency spread inside the synchronized cluster is equal to $\Delta\Omega_c = \alpha\tau\sin A$ [cf. Eq. (12)]. At $\alpha < \alpha_0$, there can be no stationary synchronized clusters. These findings are confirmed by the direct numerical simulations of Eqs. (3) and (4). In Fig. 3 the phase width of the cluster is shown for several values of $\alpha/\Delta\Omega$, and in Fig. 4 the evolution of an unstable cluster at $\alpha = 1.25 < \alpha_0$ is

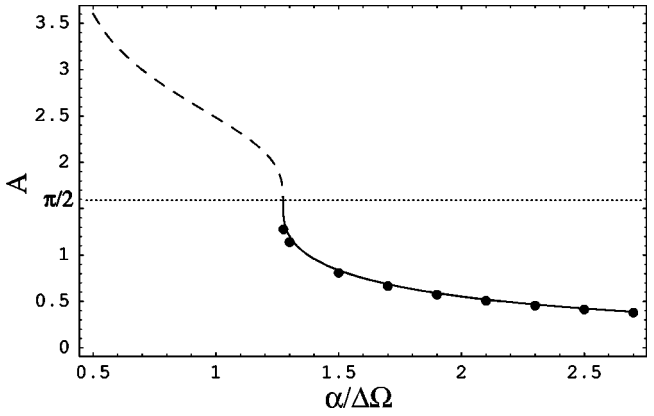

FIG. 3. Phase spread of the cluster A as a function of $\alpha/\Delta\Omega$ from Eq. (14). Dots indicate the results of numerical simulations of Eqs. (3) and (4) with 50 uniformly distributed oscillators with $\Delta\Omega = 1$, $\epsilon = 0.002$.

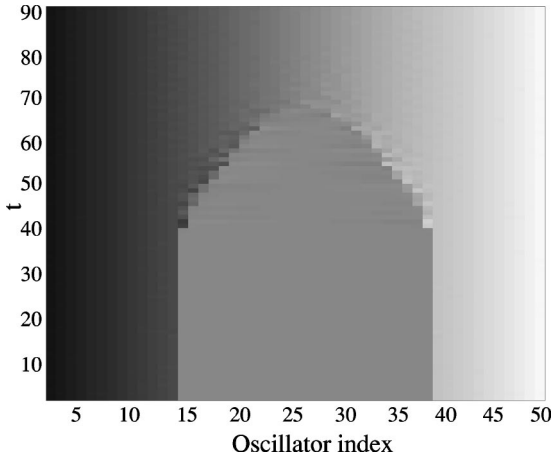

FIG. 4. Gray-scale plot of the evolution of instantaneous oscillator frequencies $\dot{\phi}_i$ for an unstable cluster at $\alpha = 1.25$ Parameters of the simulation are $N = 50$, $\epsilon = 0.002$, $\Delta\Omega = 1$. Black corresponds to $\dot{\phi} = 9.5$, and white to $\dot{\phi} = 10.5$.

shown. The parameters of simulations were $N=50$, $\Delta\Omega=1$, $\epsilon=0.002$, and the initial cluster width was chosen $\Delta\Omega_c=0.5$.

V. STABILITY OF THE CLUSTERED STATE

As we have seen in the previous section, the order parameter τ that characterizes the cluster size, can take any value from 0 to τ_{max} (for the uniform frequency distribution the latter corresponds to the whole population being synchronized, $\tau_{max}=\Delta\Omega/\alpha\sin A$). However, this is true only for small enough ϵ. Just as in the case of two coupled oscillators (Sec. III), at sufficiently large $\epsilon>\epsilon_c$, the multistability disappears, and the only stable state at $\alpha>\alpha_c$ is the one involving the whole population of oscillators, $\Delta\Omega_c=\Delta\Omega$. In order to determine ϵ_c, we analyze the following problem. Suppose we have a synchronized cluster oscillating at frequency Ω and characterized by the order parameter τ. Let us consider a single oscillator with frequency ω_0 adjacent to the cluster ($\omega_0=\Omega+\Delta\Omega_c/2$), and study its dynamics neglecting its interaction with all other oscillators and the the feedback influence of the oscillator on the cluster. Clearly, since the frequency difference between this oscillator and the cluster is smaller than that for any other non-synchronized oscillator, the adjacent oscillator will be the first to get entrained at ϵ_c. The equation for the relative phase $\psi_0=\phi_0-\Omega t$ of this oscillator reads

$$\dot{\psi}_0=\frac{\Delta\Omega_c}{2}+\frac{1}{N}\sum_{i=1}^{N_c}K_i\sin(\psi_i-\psi_0) \tag{15}$$

and the equation for the coupling coefficient between the oscillator and the ith member of the cluster,

$$\dot{K}_i=\epsilon[\alpha\cos(\psi_i-\psi_0)-K_i]. \tag{16}$$

The summation in Eq. (15) is carried only over synchronized oscillators. The phases ψ_i of the synchronized oscillators are determined by Eq. (9).

In the continuum limit for the uniform frequency distribution, these equations become

$$\dot{\psi}_0=\frac{\Delta\Omega_c}{2}+\frac{\alpha\tau}{\Delta\Omega}\int_{-A/2}^{A/2}K(\psi)\cos(2\psi)\sin(\psi-\psi_0)d\psi, \tag{17}$$

$$\dot{K}(\psi)=\epsilon[\alpha\cos(\psi-\psi_0)-K(\psi)]. \tag{18}$$

Equation (17) can be rewritten in the form

$$\dot{\psi}_0=\frac{\Delta\Omega_c}{2}+\frac{\alpha\tau}{\Delta\Omega}(P\cos\psi_0-Q\sin\psi_0), \tag{19}$$

where

$$P=\int_{-A/2}^{A/2}K(\psi)\sin\psi\cos 2\psi d\psi, \tag{20}$$

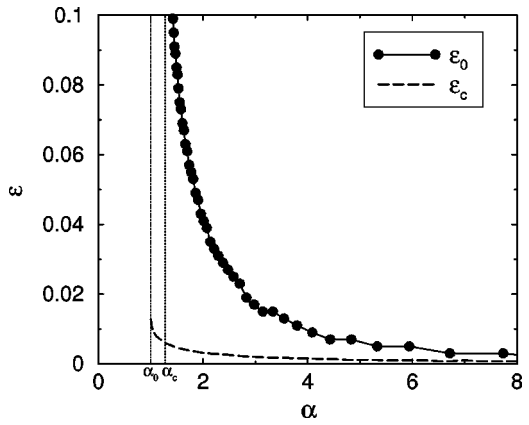

FIG. 5. Parameter plane (α,ϵ). A cluster is stable at $\alpha>\alpha_0$ and $\epsilon<\epsilon_0$. For $\alpha<\alpha_0$, clusters do not exist, for $\alpha<\alpha_0$ and $\epsilon>\epsilon_0$, cluster size increases spontaneously. Dashed line shows the stability limit for synchronization of two neighboring oscillators, for $\alpha>\alpha_c$ and $\epsilon>\epsilon_c$, random pairing of oscillators outside the main cluster occurs.

$$Q=\int_{-A/2}^{A/2}K(\psi)\cos\psi\cos 2\psi d\psi. \tag{21}$$

Equations for P,Q can be obtained using Eq. (18),

$$\dot{P}=\epsilon(\alpha F_-\sin\psi_0-P), \tag{22}$$

$$\dot{Q}=\epsilon(\alpha F_+\cos\psi_0-Q), \tag{23}$$

where $F_\pm=\frac{1}{2}\sin A\pm(\frac{1}{4}A+\frac{1}{8}\sin 2A)$. The set of equations (19),(22), and (23) exhibits the dynamics similar to Eqs. (6) for two coupled oscillators. At $\alpha<\alpha_0=4\pi^{-1}\Delta\Omega$, the only attractor of the system is the solution with periodic P and Q and unbounded phase ϕ that corresponds to ''nonentrainment'' of the oscillator by the cluster. For the phase variable taken *modulo* 2π, this solution corresponds to a limit cycle encircling the phase cylinder. At larger $\alpha>\alpha_0$, two fixed points appear, one of which (stable) corresponds to the entrainment of the oscillator by the cluster. At $\epsilon>\epsilon_0(\alpha)$, the limit cycle disappears, and the entrained state is the only stable state of the system. Thus, the critical line $\epsilon_0(\alpha)$ separates the region of cluster stability with respect to entraining additional oscillators. This line is shown in Fig. 5. This line should be compared with the critical line for pairing of two neighboring oscillators (Fig. 1). Note that we have to rescale $\tilde{\epsilon}$ and $\tilde{\alpha}$ back into original ϵ and α using $\tilde{\epsilon}=\epsilon N$, $\tilde{\alpha}=2\alpha/\Delta\Omega$. For large N, this line lies below $\epsilon_0(\alpha)$, which indicates that the random pairing outside the cluster occurs before the main cluster loses its stability. This conclusion agrees with our numerical simulations.

VI. LEARNING AND MEMORY

Information can be stored within the cluster in the form of relative phases of the oscillators in the synchronized state. Initial learning can be accomplished via driving a group of oscillators by external signals with identical frequency ω_0

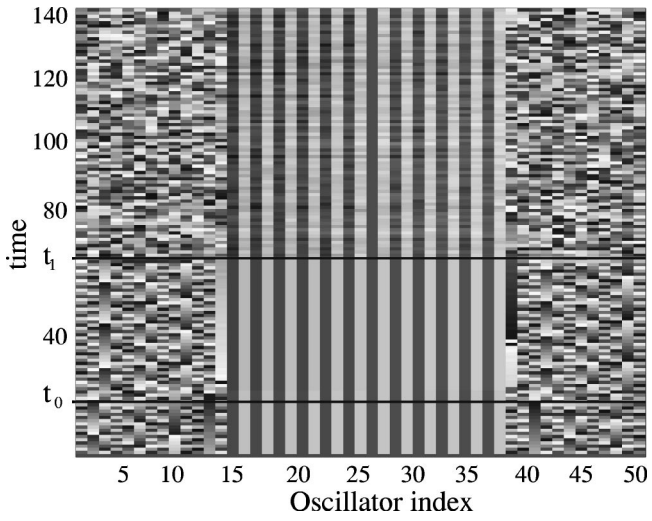

FIG. 6. Relative phase distribution of oscillators within the cluster with respect to the ''middle'' oscillator $i=25$. Gray-scale colors encode phases from 0 to 2π. The cluster is initialized by external forcing of oscillators 15-37 at frequency $\omega_0=\Omega=10.0$ for $0<t<t_0=20$. At $t>t_0$, the external forcing was turned off, but the phase distribution within the cluster survived. At $t>t_1=75$, oscillators were driven by random external fluctuation of magnitude 0.01. Despite of this forcing, the phase pattern ''memorized'' by the cluster, was preserved.

and magnitude K_0, but with different phases ϕ_i^0,

$$\dot{\phi}_i=\omega_i-\frac{1}{N}\sum_{j=1}^{N}K_{ij}\sin(\phi_i-\phi_j)+K_0\sin(\phi_i-\omega_0 t-\phi_i^0), \tag{24}$$

$$\dot{K}_{ij}=\epsilon[\alpha\cos(\phi_i-\phi_j)-K_{ij}]. \tag{25}$$

If $K_0\gg 1$, every oscillator in the group will be entrained to the external frequency ω_0. So, the external driving signals force the oscillators to oscillate in synchrony and, via slow synaptic dynamics Eq. (25), form a tightly coupled cluster. If the phases ϕ_i^0 are taken to be 0 or π, the relative phases $\phi_i-\phi_j$ within the cluster will be also close to 0 or π, and so the coupling coefficients K_{ij} will approach $\pm\alpha$. After the learning is completed after $t\approx O(\epsilon^{-1})$ time, the external signal is disconnected $(K_0\to 0)$. If the external frequency $\omega_0=\Omega$, the mean frequency of oscillators within the cluster, the cluster remains synchronized at the same frequency. Moreover, the phase relations among the oscillators are effectively preserved. Even significant random fluctuations affecting the dynamics of individual oscillators, do not change the robust structure of the synchronized cluster, see Fig. 6.

For small ϵ, after a cluster is formed, it becomes very stable with respect to external noise. Furthermore, it remains stable with respect to random variations of their natural frequencies. We let the cluster form similarly to that described above, and then at some time t_1, we perturbed the natural frequencies of all oscillators, $\omega_i=\omega_i+\Delta\omega\xi_i$, where ξ_i are independent Gaussian random variables with variance 1. We can quantify the robustness of the cluster by measuring the correlation between the synchronized cluster structure before and after the random fluctuations of natural frequencies have been applied. The correlation was calculated using the formula

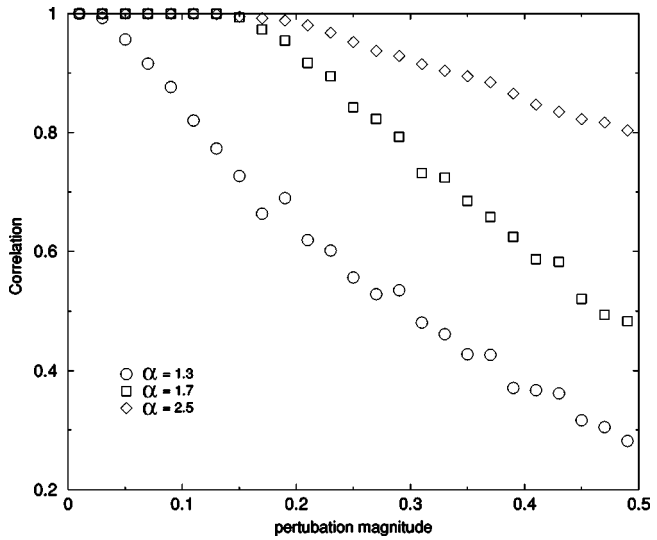

FIG. 7. Stability of cluster measured with the correlation of the cluster before and after perturbation of natural frequencies. The different curves are for several values of α, ϵ increases the stability of the cluster only slightly and falls off parallel to the curves for similar α.

$$C=\frac{\sum_{i=1}^{N}p_i\wedge q_i}{\sum_{i=1}^{N}p_i\vee q_i}, \tag{26}$$

where $p_i(q_i)$ is the binary variable describing the state of the oscillator before (after) perturbing the natural frequencies: $p_i(q_i)=1$ if the oscillator is entrained in the main cluster and $p_i(q_i)=0$ otherwise. Symbols $\vee$ and $\wedge$ denote Boolean addition and multiplication, respectively. It is easy to see that $C=1$ when the cluster remains unchanged, and $C=0$ if all oscillators leave the cluster.

Figure 7 shows correlation C as a function of the perturbation magnitude $\Delta\omega$ for several values of α. As seen in the figure, the cluster becomes more robust with the increase of α.

VII. CONCLUSION

In summary, we have demonstrated that a generalized Kuramoto model with additional equations that describe the slow dynamics of the coupling matrix can be used to elucidate the underlying mechanism of synaptic plasticity. Slow dynamics lead to multistability: synchronized clusters of different sizes and with different phase relationships among oscillators can be stabilized. The phase differences among the oscillators can be used as a way of storing and retrieving the information in this system. One natural limitation of the reduced phase description of the oscillators is that all oscilla-

tors are assumed to be in the excited (''firing'') state. However, in natural systems (such as biological neural networks), some of the neurons may be in a quiescent (''nonfiring'') state. A more general description of this system should incorporate equations for complex amplitudes of oscillators similar to Ref. [12].

We should emphasize that our model is very generic, and of course cannot be applied directly to the description of biological neurons. Nevertheless, we believe that our results may have important biological implications. In particular, they suggest that there are fundamental reasons for the wide separation of time scales of fast neuronal dynamics (e.g., membrane potential oscillations) and slow synaptic variability. They also present a very simple (possibly, the simplest) model of the *synaptic reentry reinforcement* that has been suggested to be the foundation of the long-term memory stability [1].

ACKNOWLEDGMENTS

We are indebted to M. I. Rabinovich and R. Huerta for fruitful discussions. This work was supported by the U.S. Department of Energy Grant No. DE-FG03-96ER14592 and by UC-MEXUS/CONACYT.

[1] E. Shimizu, Y.-P. Tang, C. Rampon, and J.Z. Tsien, Science **290**, 1170 (2000).
[2] L.F. Abbott and S.B. Nelson, Nat. Neurosci. **3**, 1178 (2000).
[3] D.O. Hebb, *The Organization of Behavior* (Wiley, New York, 1949).
[4] H. Markram, J. Lübke, M. Frotscher, and B. Sakmann, Science **275**, 213 (1997).
[5] L.I. Zhang, H.W. Tao, C.E. Holt, W.A. Harris, and M. Poo, Nature (London) **395**, 37 (1998).
[6] J.J. Hopfield, Proc. Natl. Acad. Sci. U.S.A. **79**, 2554 (1982).
[7] H. Tuckwell, *Introduction to Theoretical Neurobiology* (Cambridge University, Cambridge, 1988).
[8] P.D. Roberts, Phys. Rev. E **62**, 4077 (2000).
[9] H.D.I. Abarbanel, R. Huerta, and M.I. Rabinovich (unpublished).
[10] C.M. Gray, J. Comput. Neurosci. **1**, 11 (1994).
[11] H. Sompolinsky, D. Golomb, and D. Kleinfeld, Phys. Rev. A **43**, 6990 (1991).
[12] T. Aoyagi, Phys. Rev. Lett. **74**, 4075 (1995).
[13] F.C. Hoppensteadt and E.M. Izhikevich, Biol. Cybern. **75**, 129 (1996).
[14] F.C. Hoppensteadt and E.M. Izhikevich, IEEE Trans. Neural Netw. **11**, 734 (2000).
[15] A.T. Winfree, J. Theor. Biol. **16**, 15 (1967).
[16] Y. Kuramoto, *Chemical Oscillations, Waves, and Turbulence* (Springer, New York, 1984).
[17] See review by S.H. Strogatz, Physica D **143**, 1 (2000).
[18] M.K. Yueng and S.H. Strogatz, Phys. Rev. Lett. **82**, 648 (1999).
[19] F.C. Hoppensteadt and E.M. Izhikevich, Phys. Rev. Lett. **82**, 2983 (1999).